超低碳贝氏体高强度钢焊接接头强韧性表征

郭爱民[1,2]，　刘吉斌[2]，　缪　凯[2]，　董汉雄[2]，　邹德辉[2]，　贺信莱[1]
（1. 北京科技大学 材料科学与工程学院，北京　100083；2. 武汉钢铁(集团)公司 研究院，武汉　430080）

摘　要：采用焊条电弧焊、埋弧自动焊和焊接热模拟试验对控轧控冷工艺生产的超低碳贝氏体高强度厚钢板进行了焊接性能研究。结果表明，焊接热影响区具有较小的硬度差异。焊条电弧焊、埋弧自动焊实际焊接接头中热影响区硬度的最大差值小于60 HV10，与相同级别低合金高强度钢相比，焊接热影响区强度的均匀性显著提高。焊接热影响区具有高的低温冲击韧性。当焊接热输入为56 kJ/cm时，模拟过热区－40 ℃冲击吸收功可达到60 J以上。在焊条电弧焊、埋弧自动焊实际焊接工艺条件下，焊接热影响区的－40 ℃冲击吸收功可达到100 J以上。

关键词：超低碳贝氏体；焊接；热影响区；低温韧性
中图分类号：TG115.62　　文献标识码：A　　文章编号：0253－360X(2007)10－073－04


郭爱民

0　序　　言

全焊接结构和高性能参数已成为现代大型钢结构的发展方向[1]，与之相适应的易焊接高强度钢板在世界各国得到不断开发和应用，美国的ASTM A709中的HPS－70W钢和日本的SMA570W系列钢就是其中的典型钢种[2,3]。

近年来，随着钢结构快速发展，生产成本及效率已成为制约钢结构发展的关键。因此，制造业期望采用控轧控冷(thermomechanical control process，TMCP)工艺生产的具有优异焊接性能的高强度厚钢板，以替代传统调质工艺生产的高强度厚钢板。对厚钢板焊前取消预热，焊后取消消除应力热处理工序，以提高制造速率，降低生产成本。

文中介绍的新型超低碳贝氏体组织厚钢板，最大厚度达到80 mm，采用TMCP工艺生产，利用钢中的Nb元素延迟奥氏体回复和再结晶这一特性[4]，使热机械轧制过程中的奥氏体晶粒控制在较小的尺寸，充分发挥固溶Nb对钢冷却过程中相变的影响，通过控冷措施使含Nb钢得到更多的低温转变产物如针状铁素体、贝氏体等组织[5]。研制的新型高强度钢以超低碳贝氏体(ULCB)为设计主线，充分利用组织细化、控制相变等关键技术，具有高强度($R_m \geqslant$ 570 MPa)、高韧性(－40 ℃$A_{kv} \geqslant$60 J)和低焊接冷裂纹敏感性($P_{cm} \leqslant$0.18%)等综合性能特征。

作者重点介绍了新型超低碳贝氏体或针状铁素体组织厚钢板实际焊接工艺条件下，焊接接头力学性能系列试验结果，同时介绍了焊接热模拟条件下焊接热影响区力学性能的变化特征。

收稿日期：2006－12－05

1　试　　验

1.1　试验材料

试验钢板为工业生产的超低碳贝氏体钢，主要化学成分为(质量分数，%)：C0.03，Mn1.60，Si0.31，P0.014，S0.006，(Ni＋Cu＋Mo)0.6，Nb0.057。钢板工艺状态为TMCP＋回火，钢板厚度为32 mm和50 mm。采用CJ607Q超低氢焊条，熔敷金属扩散氢量为1.7 mL/100 g(水银法)。埋弧自动焊丝为WS03，焊剂为SJ101Q。钢板及焊接材料的力学性能参数见表1。

表1　试验用钢及焊接材料的力学性能参数
Table 1　Mechanical properties of tested steel

	下屈服强度 R_{eL}/MPa	抗拉强度 R_m/MPa	断后伸长率 A(%)	冲击吸收功 $A_{KV(-40\ ℃)}$/J
32 mm	555	645	20	252
50 mm	540	635	21	188
CJ607Q	560	645	27	106
WS03	555	645	27	114

1.2 焊接接头性能试验

采用埋弧自动焊对 50 mm 钢板进行试验，焊接电流 650 A，电弧电压 32 V，焊接速度 34 cm/min，焊接热输入 35 kJ/cm。焊接接头分别采用 K 形和对称 X 形坡口。对 X 形坡口进行接头常规力学性能测试，K 形坡口进行接头不同部位冲击韧性测试。

1.3 焊接热模拟试验

在 Gleeble2000 热/力动态模拟试验机上进行热影响区冲击韧性和组织特征的研究。试样尺寸为 110 mm×11 mm×11 mm。焊接热循环曲线采用 Rykalin 数学模型确定[6]，模拟厚度为 50 mm 钢板在层间温度为 150 ℃时所经历的焊接热过程：(1) 模拟不同焊接热输入的热循环曲线见图 1a，加热速度为 200 ℃/s，峰值温度为 1 350 ℃，$t_{8/5}$变化范围为 5～200 s，相当于 9～134 kJ/cm 热输入范围。(2) 模拟不同峰值温度的热循环曲线见图 1b，加热速度为 200 ℃/s，$t_{8/5}$= 20 s 相当于 34 kJ/cm 热输入，峰值温度从 1 400 ℃变化至 600 ℃，模拟基材低温回火区至过热区的力学性能变化。

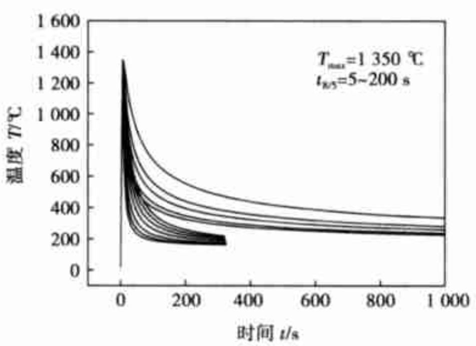

(a) 不同热输入焊接热循环曲线

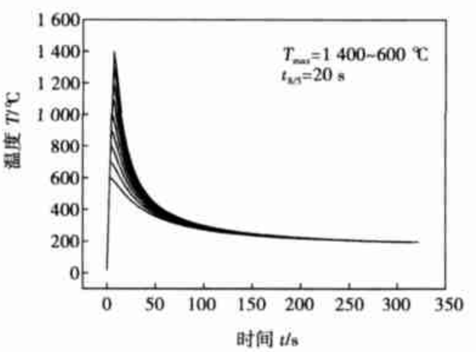

(b) 不同峰值温度焊接热循环曲线

图 1 模拟焊接热循环曲线

Fig. 1 Thermal cycling curves of simulated welding

2 试验结果与讨论

2.1 焊接热影响区强度特征

模拟不同热输入过热区硬度曲线如图 2a 所示。当 $t_{8/5}$=5 s 时，硬度值等于 239 HV10，随热输入增大过热区硬度呈降低趋势。当 $t_{8/5}$在 5～200 s 范围内，过热区的硬度值在 193～239 HV10 之间。图 2b 是模拟焊接热影响区不同峰值温度硬度曲线，揭示了热影响区不同部位强度特征。从 600 ℃开始，随着峰值温度升高，硬度值呈现出两个峰值。第一个峰值为 800 ℃，硬度值达到 216 HV10；在 900 ℃时硬度降低至 194 HV10，与基材接近。1 000～1 200 ℃之间硬度不断升高，到 1 200 ℃时达到第二个峰值，为 225 HV10。1 300～1 400 ℃过热区的硬度值为 212～214 HV10。

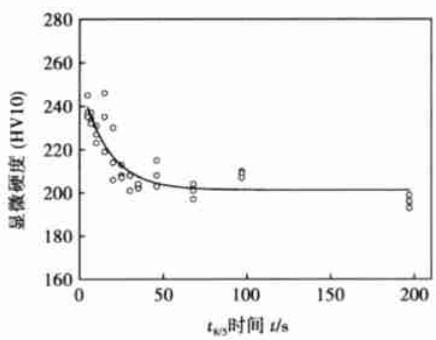

(a) 不同热输入热模拟试样硬度

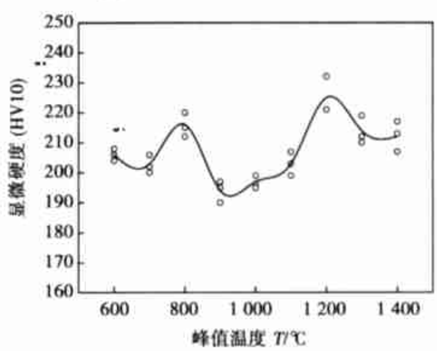

(b) 不同峰值温度热模拟试样硬度

图 2 焊接热模拟试样硬度曲线

Fig 2 Hardness profiles of simulated welding samples

埋弧自动焊焊接接头横向拉伸试样断裂位置为基材，强度达到 630 MPa，说明采用所选择的焊接材料和焊接工艺，焊接接头强度满足基材性能要求。在焊条电弧焊焊接接头过热区最高硬度达到 224 HV10，略高于埋弧自动焊相对应区域的硬度。两种工艺条件下热影响区靠近基材的区域出现较低程度的软化现象。

模拟焊接热影响区与实际焊接接头的硬度试验结果具有较好的对应性，揭示了该钢焊接热影响区的强度特点。即使在较小的焊接热输入条件下，淬硬性仍较低，在较大热输入条件下过热区未出现软化。硬度低谷出现在 900 ℃，即焊接热影响区中的

细晶区出现一定程度的软化。与调质态的 SM570Q 低合金高强度钢相比，文中所研究钢种的焊接热影响区硬度值变化小于 60 HV10，而 SM570Q 的焊接热影响区硬度变化达到 110 HV10 以上[7]。

2.2　焊接热影响区韧性特征

2.2.1　实际施焊焊接热影响区韧性特征

X 形坡口的焊条电弧焊、埋弧自动焊接头不同温度冲击韧性曲线见图 3。由图中可以看出：两种焊接工艺焊接热影响区均呈现很高的冲击韧性。焊条电弧焊热影响区－40 ℃平均冲击吸收功达到 130 J，埋弧自动焊热影响区平均冲击吸收功达到 140 J。对K形坡口埋弧自动焊接头，其焊缝、熔合线和热影响区 0.5，2，3，5 mm 等6 个位置的－30，－40 ℃低温冲击韧性曲线见图 3c。表明该钢焊接热影响区各个部位均具有很高的冲击韧性特征。

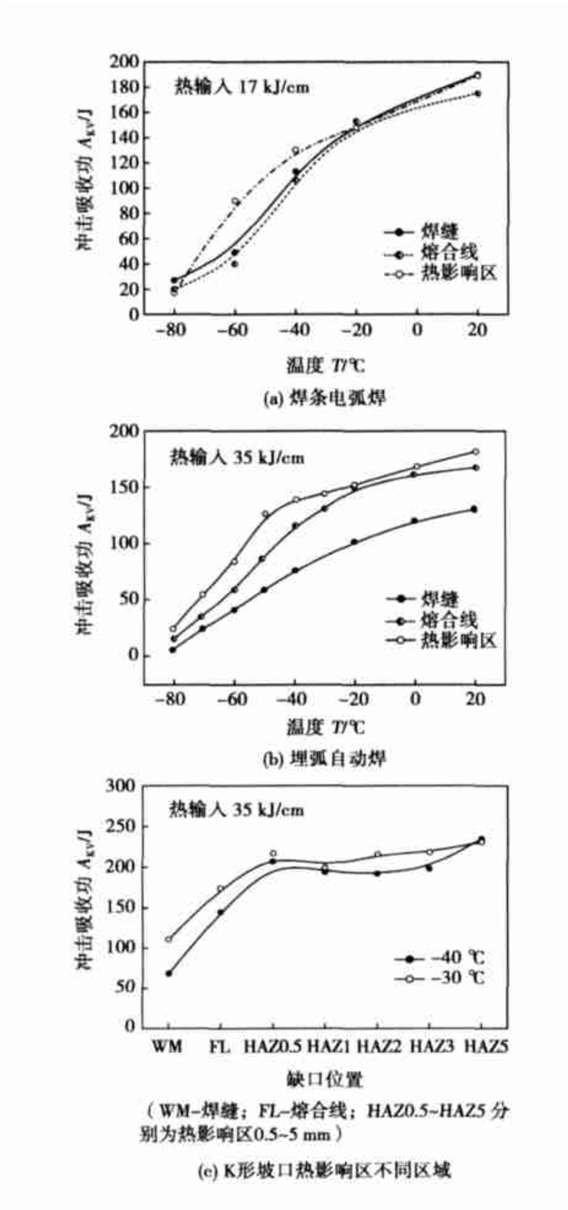

(a) 焊条电弧焊
(b) 埋弧自动焊
(c) K形坡口热影响区不同区域

图 3　焊缝与熔合线及热影响区冲击韧性曲线

Fig. 3　Impact absorbing energy at different temperatures in welding deposit, fusion line and heat-affected zone

2.2.2　热模拟焊接接头热影响区韧性特征

图 4a 给出了模拟不同热输入条件下过热区冲击韧性曲线。当 $t_{8/5}$≤20 s 时，过热区－40 ℃平均冲击吸收功达到 90 J 以上；当 $t_{8/5}$≤35 s 时，过热区－40 ℃平均冲击吸收功为 60 J 以上。对于 50 mm 钢板，如层间温度为 150 ℃，其对应的热输入分别为 34，56 kJ/cm。图 4b 为 $t_{8/5}$＝20 s 时模拟不同峰值温度的冲击韧性曲线，可以看到，在 600 ~700 ℃时，试样未达到相变温度，只经受快速回火过程，试样的冲击韧性较高。在 800 ℃时，焊接热影响区冲击韧性出现低值。900 ~1 100 ℃ 具有较高的冲击韧性，当峰值温度继续升高后，1 200 ~ 1 400 ℃间的过热区冲击韧性又出现下降。

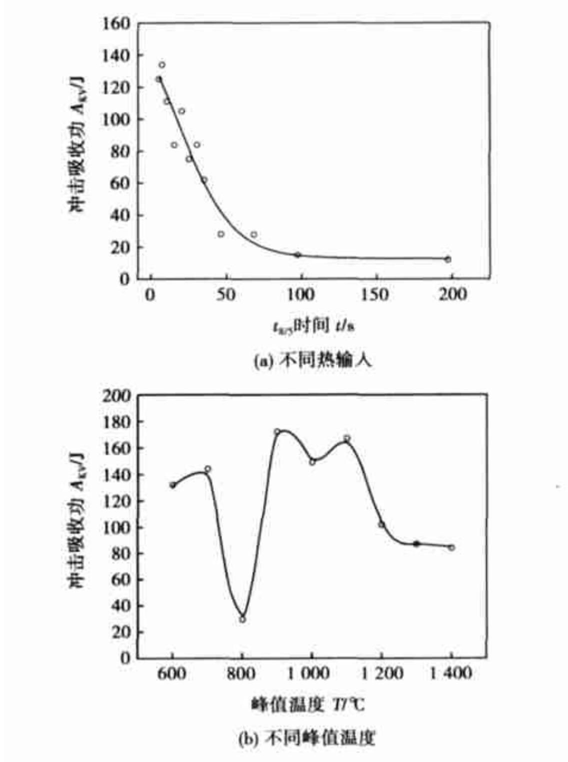

(a) 不同热输入
(b) 不同峰值温度

图 4　模拟焊接热影响区冲击韧性曲线

Fig 4　Impact absorbing energy of heat-affected zone in simulated welding samples

3　结　　论

（1）焊接热影响区具有较小的硬度差异。焊条电弧焊、埋弧自动焊实际焊接接头中热影响区硬度

的最大差值小于 60 HV10，与相同级别低合金高强度钢相比，焊接热影响区强度的均匀性显著提高。

(2) 焊接热影响区具有高的低温冲击韧性。当 $t_{8/5}$为 35 s 时(相当于 56 kJ/cm 焊接热输入)，模拟过热区−40 ℃冲击吸收功可达到 60 J 以上。焊条电弧焊、埋弧自动焊实际施焊时，焊接热影响区的−40 ℃冲击吸收功均达到 100 J 以上。但同时注意到在峰值温度 800 ℃处韧性出现低值。

参考文献：

[1] Krishna V, Karl F, William W, *et al*. Steel bridge fabrication technologies in Europe and Japan[R]. Washington DC: U.S. Department of Transportation, 2001.

[2] Caroline R K, James A S, Daniel G L. Characterization of material properties of HPS−485W(70W) TMCP for bridge girder applications[J]. Journal of Bridge Engineering, 2006, 11(1−2), 99−107.

[3] Kawabata F, Matsui K, Obinata T. Steel plates for bridge use and their application technologies[R]. Kawasaki: JFE steel corporation, 2004.

[4] Yamamoto S, Ouchi C, Osuka T. The effect of microalloying elements on the recovery and recrystallization in deformed Austenite[C] //Thermomechanical Processing of Microalloyed Austenite. Pittsburgh. 1982: 613−618.

[5] Klaus H, J M Gray. 管线钢的高温加工[C] //中信微合金化技术中心, 铌·科学与技术. 北京: 冶金工业出版社, 2003: 368−385.

[6] 牛济泰. 材料和热加工领域的物理模拟技术[M]. 北京: 国防工业出版社, 1999.

[7] Kimihiro N, Kazuyuki M, Naoyoshi T. High performance steel plates for bridge construction-high strength steel plates with excellent weldability realizing advanced design for rationalized fabrication of bridge[R]. Kawasaki: JFE Steel Corporation, 2005.

作者简介：郭爱民，男，1965 年出生。教授，博士研究生。主要研究方向为高强度结构材料及其焊接接头强韧化机制，氧化物冶金对焊接接头组织细化机理等。发表论文 30余篇。

Email：gamy007@sina.com

expands along the finer grain boundary or subgrain boundary during the solidification process. Furthermore, in 690 nickel-based alloy surfacing metal, Mn weakens the negative influence of Nb on solidification cracking resistance to some extent by restraining the segregation effect of Nb, and then the cracking resistance is improved.

Key words: 690 nickel-based alloy; solidification cracking; mechanism

Characterization on strength and toughness of welded joint for ultra-low carbon bainitic steel GUO Aimin[1,2], LIU Jibin[2], MIAO Kai[2], DONG Hanxiong[2], ZOU Dehui[2], HE Xinlai[1] (1. School of Materials Science and Engineering, Beijing University of Science and Technology, Beijing 100083, China; 2. Research and Development Institute, Wuhan Iron and Steel (Group) Company, Wuhan 430080, China). p73—76

Abstract: The weldability was investigated on ultra low-carbon bainitic steel with thermomechanical control process by utilizing shielded metal arc welding, submerged arc welding and welding thermal simulation test. Results showed that hardness is a little different in the heat affected zone (HAZ). The maximum hardness in the heat affected zone was less than 60 HV. Compared with the same class of low alloy high strength steels, the uniformity of strength in HAZ increases remarkably. The heat affected zone has high toughness. The impact absorbing energy at —40 ℃ reaches above 60 J in the simulated coarse-grained zone when the heat input was 56 kJ/cm. The impact absorbing energy at —40 ℃ reached above 100 J in shielded metal arc welding, and submerged arc welding.

Key words: ultra-low carbon bainitic steel; welding; heat affected zone; toughness

Brazing process of high temperature brazing filler metal BCo45NiCrWB LIU Enze[1,2], SUN Shuchen[1], TU Ganfeng[1], ZHENG Zhi[2], Tong Jian[2], Guo Yi[2] (1. School of Materials and Metallurgy, Northeastern University, Shenyang 110004, China; 2. Superalloys Division, Institute of Metal Research Chinese Academy of Sciences, Shenyang 110016, China). p77—80

Abstract: Wettability and flow-ability experiments of a high temperature brazing filler metal BCo45NiCrWB were studied. Dynamic analysis of brazing process was studied by a STMD-300 surface tension test apparatus. Microstructures of brazed joint with different brazing processes were studied. Microstructure of brazed joint was analyzed by optical microscope. The element distribution of brazed joint was analyzed by electron microprobe. Rupture life of brazed joint at the condition of 980 ℃/132 MPa was tested. The best brazing process of BCo45NiCrWB alloy was established. The brazing parametens are 1 220 ℃/2 h, + 1 080 ℃/4 h+ 900 ℃/16 h, all by argon quench. Results show that the high temperature brazing alloy BCo45NiCrWB has excellent process brazeability. At the condition of 980 ℃/132 MPa the rupture life is more than 60 hours.

Key words: brazing; wettability; flow-ability; rupture life

Effect of thermal cycles of DSAW on microstructure in low alloy high strength steel ZHANG Huajun, ZHANG Guangjun, WANG Junheng, WU Lin (State Key Labortory of Advanced Welding Production Technology, Harbin Institute of Technology, Harbin 150001, China). p81—84

Abstract: According to the low alloy high-strength steel thick plate welding, a new high efficiency technique which does not need back chipping—double-sided double arc welding (DSAW) was provided. Backing run with double-sided double pulsed gas metal arc welding and other passes with double-sided double gas metal arc welding. The temperature fields of single TIG (tungsten inert-gas) welding and DSAW near the bond area were measured by the method of hiding thermal-couple in drilled hole. Compared the thermal cycles of two methods, the $t_{8/5}$ and $t_{8/3}$ of DSAW are higher. In DSAW, fore pass provides the rear pass with a preheat action and rear pass provides the fore pass with a postheat treatment. In single TIG welding, microstructure of weld and coarse grain zone is coarse martensitic, but in DSAW weld contains a few of acicular ferrilite besides of martensitic. Moreover, microstructure of coarse grain zone is smaller than that of single TIG welding. Microhardness distribution results indicated that hardness of DSAW was lower than that of single TIG welding.

Key words: double-sided double arc welding; temperature field; T joint; low alloy high strength steel

Effects of heat treatment on microstructure and properties of electron beam welded TC4 titanium alloy GU Baolan, DING Dawei, WANG Li, XU Xuedong (Institute of Microstructure and Properties of Advanced Material, Beijing University of Technology, Beijing 100022, China). p85—88

Abstract: For electron beam welding (EBW) of TC4 titanium alloy with different preheat treatments and post-weld heat treatment, microstructure and phase composition characteristics of these welds of TC4 were studied by means of optical microscope and X-ray diffraction. Tension and impact test were carried out at room temperature. The results indicated that the microstructure of two kinds of base metals is the mixture of α phasse and β phase, but their state and distribution are different. The post-weld solution and aged operation carried out in the case of annealed welds leads to a coarsening and homogenous of the acicular α, the microstructures is typically reticular structure. The welds in solid solution state were given a relief annealed after welding, whose microstructure at FZ is tempered martensite α inside prior β grains and at grain boundary α. It induced that the ultimate tensile strength (UTS) of annealed state welds is less than that of solution treated welds, but the impact toughness of the former is greater than that of the latter. However, the UTS and impact toughness of these two kinds of welds are greater that that of base metal.

Key words: TC4 titanium alloy; electron beam welding; microstructure; mechanical properties

Finite element analysis simulations of life prediction for PBGA soldered joints under thermal cycling TONG Chuan, ZENG Shengkui, CHEN Yunxia (Reliability Research Institute, Beihang University, Beijing 100083, China). p89—92

Abstract: A typical plastic ball grid array (PBGA) component was selected and the plastic ball grid array packaging was modeled as a tri-layer structure composed of encapsulation, die and substrate. Visco-plastic model was used to describe the behavior of SnPb